

# Intraband absorption in finite, inhomogeneous quantum dot stacks for intermediate band solar cells: limitations and optimization

Igor Bragar and Paweł Machnikowski<sup>a)</sup>

*Institute of Physics, Wrocław University of Technology, 50-370 Wrocław, Poland*

We present a theoretical analysis of intraband optical transitions from the intermediate pseudo-band of confined states to the conduction band in a finite, inhomogeneous stack of self-assembled semiconductor quantum dots. The chain is modeled with an effective Hamiltonian including nearest-neighbor tunnel couplings and the absorption under illumination with both coherent (laser) and thermal radiation is discussed. We show that the absorption spectrum already for a few coupled dots differs from that of a single dot and develops a structure with additional maxima at higher energies. We find out that this leads to an enhancement of the overall transition rate under solar illumination by up to several per cent which grows with the number of QDs but saturates already for a few QDs in the chain. The decisive role of the strength of inter-dot coupling for the stability of this enhancement against QD stack inhomogeneity and temperature is revealed.

One of the ways to improve the efficiency of solar cells is to introduce an intermediate band in the energy spectrum of a photovoltaic structure<sup>1,2</sup>. In this way, electrons can be sequentially promoted from the valence band to the intermediate band and then to the conduction band by absorbing photons with energies below the band gap which are not converted into useful electrochemical energy in a standard structure. As an implementation of this concept, a stack of quantum dots (QDs) in the intrinsic region of a p-i-n junction solar cell has been proposed<sup>3</sup>. This idea has indeed gained some experimental support in recent years<sup>4-12</sup>. Quantum-dot-embedded p-i-n solar cells show higher quantum efficiency in near infrared range but their overall efficiency still is lower than the efficiency of similar devices without QDs<sup>4-12</sup>.

On the theory side, models involving a single QD were formulated to describe the kinetics of transitions from and into the intermediate levels<sup>13,14</sup>. On the other hand, modeling of the electron states and optical absorption in chains and arrays of QDs has been mostly limited to infinite, periodic superlattices of identical dots<sup>15-20</sup>. As we have shown recently<sup>21</sup>, enhanced absorption can appear also in finite chains of non-identical QDs but it is suppressed if the inhomogeneity of the QD chain (leading to non-identical electron ground state energies in the individual QDs) becomes too large. Since the actual QD chains are always finite (usually built of several to a few tens of QDs)<sup>4-12</sup> and unavoidably inhomogeneous it is of large practical importance for the optimal design of intermediate band photovoltaic devices to extend the theoretical analysis to such more realistic structures.

In this paper, we study the intraband optical absorption associated with the electron transition from the states confined in a finite stack of quantum dots to the conduction band. (Fig. 1) We propose a relatively simple and computation-effective model which, however, includes all the essential features of the system, in particular the inhomogeneity of the energetic parameters of the

dots forming the stack and the coupling between them. We show that the enhanced absorption features appear already for a few dots and lead to enhanced transition rate from the pseudo-band of confined states to the bulk continuum. While this effect is relatively stable with respect to inhomogeneity, it turns out to be associated with the transitions from the ground state of the stack and is washed out as soon as the temperature becomes comparable to the width of the pseudo-band of confined states. Our modeling results suggest that this detrimental temperature effect can be to a large extent overcome by increasing the tunnel coupling between the dots.

The paper is organized as follows. Sec. I defines the model of the system. In Sec. II, we briefly discuss the theoretical description of intraband transitions in the cases of coherent and thermal radiation. Next, in Sec. III, we present the results of our calculations. Sec. IV concludes the paper.

## I. MODEL

We are interested in the transitions from a single-electron bound state  $|\nu\rangle$  (with a wave function  $\Psi_\nu(\mathbf{r})$  and energy  $E_\nu$ ) to a continuum state  $|\mathbf{k}\rangle$  (with a wave function  $\Psi_{\mathbf{k}}(\mathbf{r})$  and energy  $E_{\mathbf{k}} = \hbar^2 \mathbf{k}^2 / (2m^*)$ ) (Fig. 1).

We model the confined electron states  $|\nu\rangle$  as superpositions of the ground states  $|n\rangle$  confined in the individual dots (where  $n$  numbers the dots). For simplicity, we assume that each of these single dot states has an identical wave function,

$$\psi_n(\mathbf{r}) = \psi_0(\mathbf{r} - \mathbf{R}_n),$$

where  $\mathbf{R}_n$  is the position of the  $n$ th dot (we assume that the dots are stacked along the growth direction  $z$ ). The ground state electron energies in the dots,  $\epsilon_n$ , may differ. The states  $|n\rangle$  are coupled by nearest neighbor couplings. The eigenstates  $|\nu\rangle$  and the corresponding energies  $E_\nu$  are thus obtained as the eigenstates of the effective chain Hamiltonian (assuming a single confined state in each

<sup>a)</sup>Electronic mail: Pawel.Machnikowski@pwr.wroc.pl

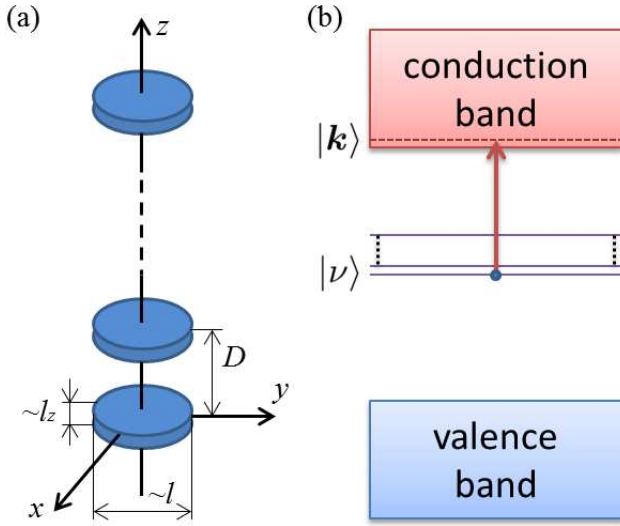


FIG. 1. (a) Sketch of a QD chain, (b) energy diagram of a QD chain with an electron transition from the bound state  $|\nu\rangle$  in the intermediate band to the state  $|\mathbf{k}\rangle$  in the conduction band.

dot)<sup>21</sup>,

$$H = \sum_{n=0}^{N-1} \epsilon_n |n\rangle\langle n| + t \sum_{n=0}^{N-2} (|n\rangle\langle n+1| + \text{h.c.}), \quad (1)$$

where  $t$  is the coupling constant. This coupling constant is determined by the barrier between the neighboring QDs. The height of the barrier depends on the band edge mismatch between the QDs and on the host materials whereas the barrier width is set in the process of growing of the QD stack. Since the stacks of self-organized QDs are produced using molecular beam epitaxy<sup>4,6,8,9,11</sup> or metal organic chemical vapor deposition<sup>5,10</sup> the barrier width (i.e. inter-dot distance  $D$ ) is controlled with a high precision up to a single monolayer, so the coupling constant  $t$  can be assumed to be the same for all pairs of neighboring QDs. We assume the overlap between the wave functions localized in different dots to be negligible, so that  $\langle n|n'\rangle = \delta_{nn'}$ . The inhomogeneity of the QD stack is taken into account by choosing the energies  $\epsilon_n$  from the Gaussian distribution with the mean  $\bar{E}$  and variance  $\sigma^2$ .

We assume that the wave function for the electron in the  $n$ th dot has the Gaussian form,

$$\psi_n(\mathbf{r}) = \frac{1}{\pi^{3/4} l_z^{1/2}} e^{-\frac{1}{2} \left[ \frac{x^2+y^2}{l^2} + \frac{(z-z_n)^2}{l_z^2} \right]},$$

where  $z_n = nD$  is the position of the  $n$ th dot and  $l, l_z$  are the extensions of the wave function in the  $xy$  plane and along  $z$ , respectively. Our choice to use the same wave function for all QDs which have not necessarily the same ground energy levels can be argued as follows. Using

the model of quantum harmonic oscillator we can estimate that small differences of the confined energy levels in a QD (of the order of a few meV) correspond to very small changes of the parameters of the wave function (of the order of a few percent), so we can approximate wave function of each QD by a Gaussian function with constant parameters  $l$  and  $l_z$ . On the other hand, when the differences of the QD confined level energies are larger strong localization of an electron on the QD with the lowest energy level occurs, which means that the exact form of the wave functions (i.e. knowledge of the precise values of parameters) of other QDs become irrelevant, so that in this case we also can use the same parameters  $l$  and  $l_z$  for all QDs of the chain.

For the bulk electron states, we assume plane waves<sup>22</sup> orthogonalized to the localized states, as previously proposed for calculating carrier capture rates<sup>23-25</sup>. These states are labeled by the wave vector  $\mathbf{k}$  describing the plane wave far away from the QD structure. Thus, we have

$$\Psi_{\mathbf{k}}(\mathbf{r}) = N_{\mathbf{k}} \left[ \frac{1}{\sqrt{V}} e^{i\mathbf{k}\cdot\mathbf{r}} - \sum_n \gamma_{\mathbf{k}n} \psi_n(\mathbf{r}) \right],$$

where  $N_{\mathbf{k}}$  is the appropriate normalization constant, we assume normalization in a box of volume  $V$  with periodic boundary conditions, and the orthogonalization coefficients  $\gamma_{\mathbf{k}n}$  are given by

$$\gamma_{\mathbf{k}n} = \frac{1}{\sqrt{V}} \int d^3r \psi_n^*(\mathbf{r}) e^{i\mathbf{k}\cdot\mathbf{r}} = e^{ik_z z_n} \gamma_{\mathbf{k}0},$$

where

$$\gamma_{\mathbf{k}0} = \frac{l_z^{1/2} \pi^{3/4} 2^{3/2}}{\sqrt{V}} e^{-\frac{1}{2} [l^2 (k_x^2 + k_y^2) + l_z^2 k_z^2]}.$$

The coupling of carriers to the incident light is described by the dipole Hamiltonian

$$H_{\text{int}} = e\mathbf{r} \cdot \mathcal{E}(\mathbf{r}), \quad (2)$$

where  $e$  is the elementary charge and  $\mathcal{E}$  is the electric field. We will consider two cases: A monochromatic laser light will be described as a classical plane wave field

$$\mathcal{E}^{(\text{cl})}(\mathbf{r}) = \frac{1}{\epsilon_0 \epsilon_\infty} \hat{\mathcal{E}} \mathcal{E}_0 \cos(\mathbf{q} \cdot \mathbf{r} - \omega_q t), \quad (3)$$

where  $\epsilon_0$  is the vacuum permittivity,  $\epsilon_\infty$  is the high-frequency dielectric constant of the semiconductor,  $\mathcal{E}_0$  is the amplitude of the electric field of the electromagnetic wave,  $\hat{\mathcal{E}}$  is a unit vector defining its polarization,  $\mathbf{q}$  is its wave vector (inside the dielectric medium), and  $\omega_q = cq/n_r$  is its frequency, where  $n_r$  is the refractive index of the semiconductor. On the other hand, for thermal radiation, corresponding to the natural working conditions of a solar cell, the field is

$$\mathcal{E}^{(\text{th})}(\mathbf{r}) = \sum_q' \sqrt{\frac{\hbar \omega_q}{2\epsilon_0 \epsilon_\infty V}} \hat{\mathcal{E}} a_q e^{i\mathbf{q}\cdot\mathbf{r}} + \text{h.c.}, \quad (4)$$

where  $a_{\mathbf{q}}$  is the annihilation operator for a photon with the wave vector  $\mathbf{q}$ ,  $V$  is the formal normalization volume, and we take into account that the incident solar radiation is propagating into a specific direction, hence its wave vectors are distributed over a very small solid angle around its direction of propagation  $\hat{\mathbf{q}}$  (which is represented by the prime at the summation sign). For more flexibility of the modeling, we assume also that the radiation is polarized (the effects of unpolarized radiation can be modeled by averaging over the directions of polarization).

## II. LIGHT ABSORPTION BY A QD CHAIN

In the description of light induced transitions from the confined states to the extended states we assume that the occupation of the latter is negligible, which in a solar cell corresponds to assuming efficient carrier collection.

In the case of classical (coherent) monochromatic light with frequency  $\omega$ , propagation direction  $\hat{\mathbf{q}}$ , and polarization  $\hat{\mathcal{E}}$ , the transition rate from a state  $|\nu\rangle$  to the continuum of extended states is obtained in the usual way from the Fermi golden rule<sup>26</sup> using the interaction Hamiltonian (1) with the field given by Eq. (3),

$$\alpha_{\nu}(\omega, \hat{\mathbf{q}}, \hat{\mathcal{E}}) = \frac{2\pi}{\hbar^2} \left( \frac{e\mathcal{E}_0}{2\varepsilon_0\varepsilon_{\infty}} \right)^2 \sum_{\mathbf{k}} \left| \langle \Psi_{\mathbf{k}} | \mathbf{r} \cdot \hat{\mathcal{E}} e^{i\mathbf{q}\cdot\mathbf{r}} | \Psi_{\nu} \rangle \right|^2 \delta(\omega - \omega_{\mathbf{k}\nu}).$$

where  $\omega_{\mathbf{k}\nu} = (E_{\mathbf{k}} - E_{\nu})/\hbar$ . This can be written in the form

$$\alpha_{\nu}(\omega, \mathbf{q}, \hat{\mathcal{E}}) = \frac{\pi e^2 \mathcal{U}}{\hbar^2 \varepsilon_0 \varepsilon_{\infty}} \sum_{\mathbf{k}} |\alpha_{\nu\mathbf{k}}(\mathbf{q})|^2 \delta(\omega - \omega_{\mathbf{k}\nu}), \quad (5)$$

where  $\mathcal{U} = \varepsilon_0 \varepsilon_{\infty} E_0^2 / 2$  is the energy density of the electromagnetic wave and

$$\alpha_{\nu\mathbf{k}}(\mathbf{q}) = \int d^3r \Psi_{\mathbf{k}}^*(\mathbf{r}) e^{i\mathbf{q}\cdot\mathbf{r}} \mathbf{r} \cdot \hat{\mathcal{E}} \Psi_{\nu}(\mathbf{r}). \quad (6)$$

In the case of illumination by broad band thermal radiation, we first use the Hamiltonian (2) with the quantum field given by Eq. (4) to calculate the Fermi golden rule probability of absorption of a photon with a wave vector  $\mathbf{q}$ ,

$$\gamma_{\nu}(\mathbf{q}) = \frac{2\pi}{\hbar} \sum_{\mathbf{k}} \frac{e^2 \hbar \omega_{\mathbf{q}}}{2\varepsilon_0 \varepsilon_{\infty}} |\alpha_{\nu\mathbf{k}}(\mathbf{q})|^2 n_{\mathbf{q}} \delta(\omega_{\mathbf{q}} - \omega_{\mathbf{k}\nu}),$$

where  $n_{\mathbf{q}}$  is the Bose distribution of photon occupations at the temperature of solar black body radiation and the transition matrix elements  $\alpha_{\nu\mathbf{k}}(\mathbf{q})$  are given by Eq. (6). We note that for radiation propagating in a fixed direction  $\hat{\mathbf{q}}$ , the overlap integral  $\alpha_{\nu\mathbf{k}}(\mathbf{q})$  actually depends only on the frequency,  $\alpha_{\nu\mathbf{k}}(\mathbf{q}) = \alpha_{\nu\mathbf{k}}(n\omega_{\mathbf{q}}\hat{\mathbf{q}}/c)$ . Then, the total photon absorption rate for an initial confined state

$|\nu\rangle$  per unit frequency interval is

$$\begin{aligned} \beta_{\nu}(\omega, \hat{\mathbf{q}}, \hat{\mathcal{E}}) &= \sum_{\mathbf{q}}' \delta(\omega - \omega_{\mathbf{q}}) \gamma_{\nu}(\mathbf{q}) \\ &= \sum_{\mathbf{k}} \left| \alpha_{\nu\mathbf{k}} \left( \frac{n\omega_{\mathbf{q}}}{c} \hat{\mathbf{q}} \right) \right|^2 \frac{\pi e^2}{\hbar \varepsilon_0 \varepsilon_{\infty}} \delta(\omega_{\mathbf{q}} - \omega_{\mathbf{k}\nu}) \\ &\quad \times \frac{1}{V} \sum_{\mathbf{q}}' \hbar \omega_{\mathbf{q}} n_{\mathbf{q}} \delta(\omega - \omega_{\mathbf{q}}). \end{aligned}$$

The final sum in this expression is the spectral distribution of the energy density of radiation  $u(\omega)$  which, for solar light, is approximately described by the Planck law. Hence, the absorption rate under illumination by thermal radiation can be written in the form analogous to Eq. (5),

$$\beta_{\nu}(\omega, \hat{\mathbf{q}}, \hat{\mathcal{E}}) = \frac{\pi e^2 u(\omega)}{\hbar \varepsilon_0 \varepsilon_{\infty}} \sum_{\mathbf{k}} |\alpha_{\nu\mathbf{k}}(\mathbf{q})|^2 \delta(\omega - \omega_{\mathbf{k}\nu}). \quad (7)$$

Eqs. (5) and (7), along with the effective chain Hamiltonian (1), are the basis for numerical calculations the results of which are presented in the next section.

## III. RESULTS

In this section, we present results of numerical calculations of the intraband absorption in QD chains using the approach described in Sec. I and Sec. II.

In all our simulations we focus on an InAs/GaAs structure (not optimal for a solar cell<sup>1</sup> but important for the current laboratory scale investigations<sup>2</sup>). We assume the wave function confinement sizes  $l = 4.5$  nm,  $l_z = 1.0$  nm (see Ref. 21 for the discussion of the dependence on these parameters),  $\bar{E} = -250$  meV. Based on earlier  $\mathbf{k} \cdot \mathbf{p}$  calculations<sup>27</sup>, the tunnel coupling  $t$  is given by the formula

$$\ln \frac{t}{t_0} = -\mathcal{K}D,$$

where  $\mathcal{K} = 0.59$  nm<sup>-1</sup>,  $t_0 = 0.79$  eV ( $t = -3.9$  and  $-41.3$  meV for  $D = 9$  and  $5$  nm, respectively).

In Fig. 2(a), we show the intraband absorption spectra of short chains of identical QDs compared to the spectrum of a single dot for light incident along the chain (in the  $z$  direction) and perpendicular to the chain. Both spectra are calculated assuming that only the lowest confined state is considerably occupied (which corresponds to low temperatures) and for unpolarized light (for perpendicular incidence, the contribution from light polarized along  $z$  is small). In both cases, the absorption spectrum for a single dot shows only a single maximum with a long tail on the high energy side but already for a few dots it develops a series of additional maxima. As can be seen in Fig. 2(b), the spectra for a chain of 10 QDs smoothly evolve between the two limiting geometries as the incidence angle is tilted from normal to in-plane incidence.

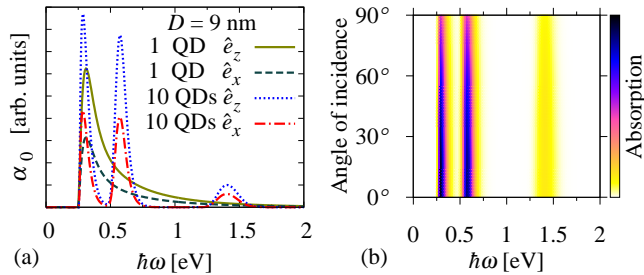


FIG. 2. (a) Low temperature intraband absorption spectra for a chain of identical dots illuminated by coherent monochromatic unpolarized light incident along and perpendicular to the stacking direction  $z$  (as indicated by  $\hat{e}_z$  and  $\hat{e}_x$ , respectively). (b) The dependence of the spectrum on the angle of incidence for 10 QDs.

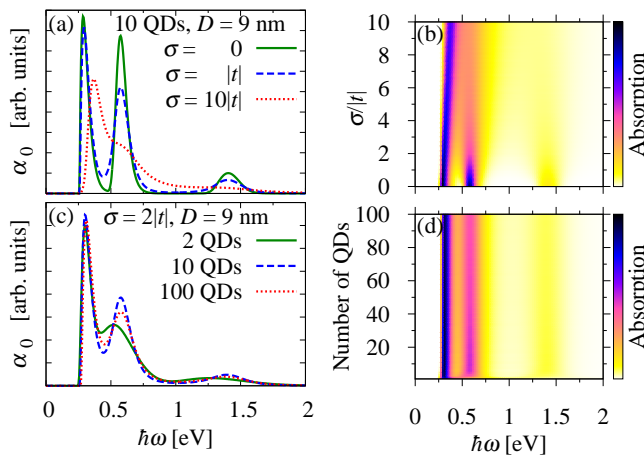


FIG. 3. Low temperature intraband absorption spectrum for a chain of non-identical dots illuminated by coherent monochromatic unpolarized light incident along the stacking direction  $z$ . (a,b) As a function of the degree of inhomogeneity; (c,d) as a function of the chain length. Each spectrum is an average of 1000 realization with randomly chosen values of  $\epsilon_n$ .

The additional absorption peaks that can be seen in Fig. 2 result from interference effects which are due to delocalization of the electron state and lead to preferred transitions to states with  $k_z = 2\pi j/D$ , where  $j$  is an integer<sup>21</sup>. Disorder, which in our case has the form of inhomogeneity of the “on-site” energies  $\epsilon_n$ , destroys the coherently delocalized electron states and leads to localization. As a result, the additional peaks are suppressed and the absorption spectrum becomes more similar to that of a single dot (see Fig. 3(a,b)). As we show in Fig. 3(c,d), while the spectra for QD stacks differ considerably from those for a single dot, the extension of the stack above 10 dots has little effect. Note that the effect of interference of transition amplitudes depends to some extent on whether their magnitudes are equal or not. Hence, if one allows different geometries of wave func-

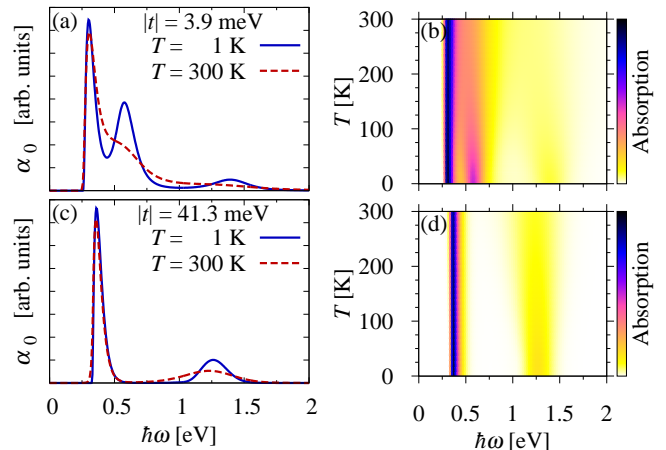


FIG. 4. Intraband absorption spectrum for a chain of 10 non-identical dots with  $\sigma = 7.8$  meV, illuminated by coherent monochromatic unpolarized light incident along the stacking direction  $z$  as a function of temperature for two values of the inter-dot coupling: (a,b)  $t = -3.9$  meV (corresponding to  $D = 9$  nm), (c,d)  $t = -41.3$  meV (corresponding to  $D = 5$  nm).

tions in non-identical QDs then additional suppression of the interference-related additional peaks may occur. However, this effect is expected to be small compared to the suppression due to localization.

For a realistic device, absorption at elevated temperatures is relevant. At non-zero temperatures, the occupation of excited states in the QD-related pseudo-band is non-negligible, which leads to a reconstruction of the spectrum, as shown in Fig. 4. For chains with  $|t| < kT$ , the structure of the spectrum is washed away with increasing temperature (Fig. 4(a,b)). However, as can be seen from Fig. 4(c,d) strong coupling broadens the pseudo-band beyond the thermal energies and stabilizes the chain absorption against temperature.

In order to study the properties of the device under realistic working conditions we calculate also the electron intraband transition rate  $\beta_0$  (from the ground state) for a chain of non-identical QDs illuminated by black body radiation. The energy density of radiation with  $T = 5777$  K was normalized to the incident flux of  $1 \text{ kW/m}^2$  (one sun). In Fig. 5(a,b) we show the spectral distribution of the transition rates as a function of the energy of the absorbed photon. Comparison with the absorption spectra shown in Fig. 2 shows that the qualitative form of these two spectral characteristics is similar but quantitatively the transition rate at higher photon energies is enhanced relative to that at lower energies. This is due to the very quickly growing spectral densities of the thermal photon field at higher energies (according to the the Planck law) which enhances the role of higher energy photons (and, in consequence, the overall absorption of energy in the corresponding spectral range). One should notice that inhomogeneity (higher values of  $\sigma$ ) leads to a less struc-

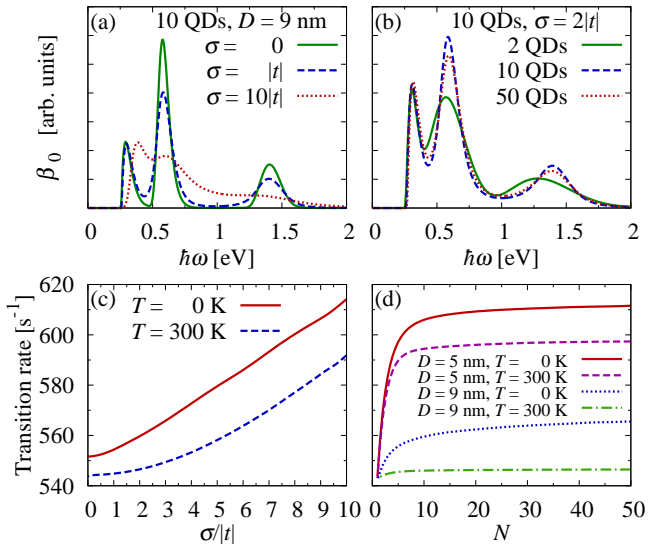


FIG. 5. (a,b) Electron intraband transition rates under illumination by one sun thermal radiation as a function of the degree of inhomogeneity (a) and as a function of the number of QDs in the chain (b). Each spectrum is an average of 1000 realization with randomly chosen values of  $\epsilon_n$ . (c,d) Integrated single-electron transition rate under illumination by one sun thermal radiation as a function of the degree of inhomogeneity (c) and as a function of the number of QDs in the chain(d).

tured spectrum with non-vanishing absorption over all the spectral range.

In fig Fig. 5(c), we show the total transition rate, integrated over photon energies. The result at 300 K includes the thermal distribution of the initial states of the electron. As one can see, the total rate increases as the inhomogeneity grows. This increase is due to the increasing probability that the electron will localize in a dot with much lower “on-site” energy as the QD energy distribution broadens. This enhances the transition rate because of the growing spectral density of radiation for higher energy differences between the initial and final states. As a function of the chain length (Fig. 5(d)), the total transition rate increases slightly (up to several %) for strongly coupled chains at low temperatures and then saturates for  $N \gtrsim 10$ . This increase is mostly due to high-frequency contributions corresponding to the enhanced high-energy absorption features in a QD stack (cf. Fig. 2). One can notice in Fig. 5(d) that the gain in the total transition rate for strongly coupled dots not only is much larger than for weaker coupling but it is also much less sensitive to temperature.

#### IV. CONCLUSIONS

We have proposed a model which describes electron states and intraband absorption spectra which corre-

spond to the transitions from the QD pseudo-band to the conduction band. We have studied the absorption spectra as a function of the degree of inhomogeneity, the number of QDs in the chain, the inter-dot separation, the temperature and the illumination conditions. We have shown that the absorption spectrum even of short QD chains (a few QDs) is dominated by interference effects that leads to the appearance of additional absorption maxima and does not considerably evolve further if the chain length exceeds approximately 10 dots. The overall transition rate under illumination with black body radiation increases by up to several per cent with the number of QDs but also saturates already for a few QDs in the chain. The structured absorption spectrum persists when the inhomogeneity of the QD transition energies is increased up to the values comparable with the magnitude of the inter-dot coupling. Strong coupling between the dots is essential for maintaining the chain absorption features up to high temperatures. On practical side, our results show that already a stack of a few QDs manifests the absorption features characteristic of QD chains and that these features are stable against temperatures and energy inhomogeneities if the dots are sufficiently strongly coupled. However, a QD chain shows only a slightly increases absorption as compared to a single dot and the increase of absorption is dominated by high-energy photons, which may lead to competition with the interband absorption. Moreover, a trade-off has to be found between the absorption enhancement in strongly coupled chains and the need to reduce tunneling in order to avoid carrier escape from the intermediate bands<sup>28</sup>.

#### ACKNOWLEDGMENTS

This work was funded from the TEAM programme of the Foundation for Polish Science, co-financed by the European Regional Development Fund.

- <sup>1</sup>A. Luque and A. Martí, Phys. Rev. Lett. **78**, 5014 (1997).
- <sup>2</sup>A. Luque, A. Martí, and C. Stanley, Nat. Phot. **6**, 146 (2012).
- <sup>3</sup>V. Aroutiounian, S. Petrosyan, A. Khachatryan, and K. Tourian, J. Appl. Phys. **89**, 2268 (2001).
- <sup>4</sup>R. B. Laghumavarapu, A. Moscho, A. Khoshakhlagh, M. El-Emawy, L. F. Lester, and D. L. Huffaker, Appl. Phys. Lett. **90**, 173125 (2007).
- <sup>5</sup>S. M. Hubbard, C. D. Cress, C. G. Bailey, R. P. Raffaele, S. G. Bailey, and D. M. Wilt, Appl. Phys. Lett. **92**, 123512 (2008).
- <sup>6</sup>R. Oshima, A. Takata, and Y. Okada, Appl. Phys. Lett. **93**, 083111 (2008).
- <sup>7</sup>Y. Okada, R. Oshima, and A. Takata, J. Appl. Phys. **106**, 024306 (2009).
- <sup>8</sup>Y. Okada, T. Morioka, K. Yoshida, R. Oshima, Y. Shoji, T. Inoue, and T. Kita, J. Appl. Phys. **109**, 024301 (2011).
- <sup>9</sup>S. A. Blokhin, A. V. Sakharov, A. M. Nadtochy, A. S. Pauysov, M. V. Maximov, N. N. Ledentsov, A. R. Kovsh, S. S. Mikhlin, V. M. Lantratov, S. A. Mintairov, N. A. Kaluzhniy, and M. Z. Shvarts, Fiz. Tekh. Poluprovodn. **43**, 537 (2009), [Semiconductors **43**, 514 (2009)].
- <sup>10</sup>D. Guimard, R. Morihara, D. Bordel, K. Tanabe, Y. Wakayama, M. Nishioka, and Y. Arakawa, Appl. Phys. Lett. **96**, 203507 (2010).

- <sup>11</sup>X. Shang, J. He, H. Wang, M. Li, Y. Zhu, Z. Niu, and Y. Fu, *Appl. Phys. A* **103**, 335 (2011).
- <sup>12</sup>X.-J. Shang, J.-F. He, M.-F. Li, F. Zhan, H.-Q. Ni, Z.-C. Niu, H. Pettersson, and Y. Fu, *Appl. Phys. Lett.* **99**, 113514 (2011).
- <sup>13</sup>A. Luque, A. Martí, E. Antolín, and P. Garcia-Linares, *Sol. Energ. Mater. Sol. C.* **94**, 2032 (2010).
- <sup>14</sup>A. Luque, A. Martí, E. Antolín, P. G. Linares, I. Tobías, I. Ramiro, and E. Hernandez, *Sol. Energ. Mater. Sol. C.* **95**, 2095 (2011).
- <sup>15</sup>Q. Shao, A. A. Balandin, A. I. Fedoseyev, and M. Turowski, *Appl. Phys. Lett.* **91**, 163503 (2007).
- <sup>16</sup>S. Tomić, T. S. Jones, and N. M. Harrison, *Appl. Phys. Lett.* **93**, 263105 (2008).
- <sup>17</sup>S. Tomić, *Phys. Rev. B* **82**, 195321 (2010).
- <sup>18</sup>J. W. Kłos and M. Krawczyk, *J. Appl. Phys.* **106**, 093703 (2009).
- <sup>19</sup>J. W. Kłos and M. Krawczyk, *J. Appl. Phys.* **107**, 043706 (2010).
- <sup>20</sup>Q. Deng, X. Wang, C. Yang, H. Xiao, C. Wang, H. Yin, Q. Hou, J. Li, Z. Wang, and X. Hou, *Physica B* **406**, 73 (2011).
- <sup>21</sup>I. Bragar and P. Machnikowski, *Acta Phys. Polon. A* **120**, 862 (2011).
- <sup>22</sup>I. Magnusdottir, A. V. Uskov, S. Bischoff, B. Tromborg, and J. Mørk, *J. Appl. Phys.* **92**, 5982 (2002).
- <sup>23</sup>R. Ferreira and G. Bastard, *Appl. Phys. Lett.* **74**, 2818 (1999).
- <sup>24</sup>H. C. Schneider, W. W. Chow, and S. W. Koch, *Phys. Rev. B* **64**, 115315 (2001).
- <sup>25</sup>T. R. Nielsen, P. Gartner, and F. Jahnke, *Phys. Rev. B* **69**, 235314 (2004).
- <sup>26</sup>A. Messiah, *Quantum Mechanics* (North-Holland, Amsterdam, 1966).
- <sup>27</sup>K. Gawarecki, M. Pochwała, A. Grodecka-Grad, and P. Machnikowski, *Phys. Rev. B* **81**, 245312 (2010).
- <sup>28</sup>E. Antolín, A. Martí, C. D. Farmer, P. G. Linares, E. Hernández, A. M. Sánchez, T. Ben, S. I. Molina, C. R. Stanley, and A. Luque, *J. Appl. Phys.* **108**, 064513 (2010).